Atom Indonesia

Journal homepage: https://atomindonesia.brin.go.id

Characterizing Photon Beam Properties of a TrueBeam STx Linear Accelerator: An Evaluation of Geant4/GATE Monte Carlo Simulation Tool Performance

P. H. Lam[1,2], P. T. Dung[3], P. Q. Trung[4*]

[1]*Military Hospital 103, 261 Phung Hung, Ha Dong, Hanoi 12108, Viet Nam*
[2]*Viet Nam Academy of Science and Technology (VAST), 18 Hoang Quoc Viet, Cau Giay, Hanoi 11355, Viet Nam*
[3]*Institute of Material Sciences, 18 Hoang Quoc Viet, Cau Giay, Hanoi 11355, Viet Nam*
[4]*Radiation Oncology and Radiosurgery Department, 108 Military Central Hospital, 1 Tran Hung Dao, Hai Ba Trung, Hanoi 11600, Viet Nam*

ARTICLE INFO

Article history:
Received 5 April 2024
Received in revised form 27 June 2024
Accepted 27 June 2024

Keywords:
Photon beam
FF and FFF
Monte carlo simulation
Geant4/GATE.

ABSTRACT

Purpose: This study aims to investigate the characteristics of photon beams from TrueBeam STx, comparing flattening filter (FF) and flattening filter free (FFF) configurations between measurements and Monte Carlo simulation. Instruments and methods: The Geant4/GATE simulation toolkit was utilized to simulate percentage depth dose (PDD), off-axis distance profiles (profiles), d_{max}, $TPR_{20/10}$, surface dose, field size, penumbra, flatness, and symmetry. Subsequently, these simulated results were compared with experimental measurements and evaluated using the gamma index method. Results: There was a good agreement between simulation and experimental measurement results in modeling the PDD and profile of photon beams. All gamma passing rate indices exceeded 97 %, 94 %, and 90 % with criteria of 3 % and 3 mm, 2 % and 2 mm, and 1 % and 1 mm, respectively. The calculated results of beam characteristics (d_{max}, $TPR_{20/10}$, surface dose, field size, penumbra, flatness, and symmetry) were highly compatible with experimental measurements, with discrepancies less than 3 %, except for the surface dose of the 6MV FF photon beam, which had an error of 3.83 %. Conclusion: The Geant4/GATE simulation toolkit provided accurate results for simulating and investigating photon beam characteristics, aligning closely with experimental measurements.

INTRODUCTION

The TrueBeam STx, developed by Varian Medical Systems in the USA, is an advanced system in radiation therapy for precise tumor treatment. It integrates image-guided radiosurgery and radiotherapy technologies, and clinicians can administer highly accurate and effective treatment. The TrueBeam STx offers a comprehensive array of treatment modalities, including stereotactic radiosurgery (SRS), stereotactic body radiation therapy (SBRT), intensity-modulated radiation therapy (IMRT), and image-guided radiation therapy (IGRT) [1,2].

Distinguished by its sophisticated motion management capabilities, the TrueBeam STx accommodates tumor and patient motion during treatment, ensuring precise dose delivery while safeguarding healthy surrounding tissues. Furthermore, the TrueBeam STx Linac have a multi-energy configuration capable of delivering photon and electron beams at various energy levels. Notably, besides the flattened filtered (FF) photon beam, the Linac offers the flattened filtered-free (FFF) photon beam mode, a standout feature of this device. The physics characteristics of flattened filter-free photon beams render them particularly

*Corresponding author.
E-mail address: qtphamhus@gmail.com
DOI: https://doi.org/10.55981/aij.2024.1451

suitable, convenient, and widely utilized in clinical practice.

Photon beams possess numerous advanced characteristics that make them well-suited for application in radiotherapy. Dosimetry characteristics of clinical photon beams are typically represented by parameters such as percentage depth dose (PDD), off-axis distance dose (profile), and additional dosimetry parameters including output factor, dose rate, and wedge factor, among others. Common beam characteristics encompass d_{max}, $TPR_{20/10}$, flatness, symmetry, penumbra, field size, surface dose, out-of-field dose, output factor, and dose rate.

These dosimetry properties are influenced by factors such as photon energy, beam fluence, Linac head geometry, and material composition. Understanding these characteristics is pivotal for optimizing treatment planning processes, ensuring the safe and effective delivery of doses to the target area, and minimizing radiation exposure to healthy tissues.

The Monte Carlo (MC) method offers insights that cannot be obtained through direct measurement or analytical calculations. In the field of radiotherapy, Monte Carlo methods find application in radiation dosimetry, treatment planning, quality assurance (QA), and the design of treatment devices [3-5]. Numerous Monte Carlo simulation tools are currently in widespread use, including PENELOPE, MCNP, EGSnrc, Geant4, GATE, and PHITS.

GATE, a Monte Carlo simulation toolkit built upon Geant4, is specifically designed to simulate the behavior of particles as they traverse through matter. Initially utilized in medical physics applications, particularly in emission tomography, GATE has since undergone continued development and has found extensive applications in radiotherapy and radiobiology. It has significantly contributed to photon beam modeling of radiotherapy linear accelerators, dose calculations, treatment planning, and research endeavors [6].

Several researchers have delved into studying the characteristics of radiotherapy accelerator photon beams through various methods including experimental measurements, calculations, or Monte Carlo simulation tools. For instance, Asghar Mesbahi evaluated the dosimetry properties of a 6 MV FFF photon beam from a Varian Clinac 21EX Linac using the MCNP4C code [7]. Similarly, Maged Mohammed et al. conducted a comparative evaluation of the dosimetry properties of 6 MV FF and FFF photon beams from a Varian 2100 Linac using the EGSnrc code [8]. Esin Gündem et al. analyzed and validated the characteristics of a 6 MV photon beam produced by an Elekta Synergy Linac using the EGSnrc code [9]. Additionally, Achir Sara et al. examined the dosimetry characteristics of both 6 MV FF and FFF photon beams from the TrueBeam Linac, utilizing statistical analysis with the Kruskal-Wallis H test [10].

Although Monte Carlo simulation tools are widely used in radiotherapy research, a comprehensive study of the full clinical photon beams of the TrueBeam STx Linac using the GATE simulation toolkit is still lacking. Geant4/GATE offers advantages such as modularity, flexibility, and precise modeling of complex geometries and physical processes. This study aims to fill this gap by using Geant4/GATE to investigate the dosimetry characteristics of photon beams from the TrueBeam STx Linac. We compare dosimetric parameters, including d_{max}, $TPR_{20/10}$, surface dose, symmetry, flatness, and penumbra, between Monte Carlo simulations and experimental measurements, focusing on six clinically relevant photon beams, including 6, 8, 10, and 15 MV FF beams, and 6 and 10 MV FFF beams. This study seeks to validate and assess the TrueBeam STx Linac's performance with Geant4/GATE, offering valuable insights for improving clinical practices in radiotherapy.

METHODOLOGY

The validation of photon beam

The measurements

The measurements were conducted using photon beams sourced from a TrueBeam STx linear accelerator (Varian, USA), located at the 108 Military Center Hospital, Viet Nam. A water phantom (IBA Blue phantom, Germany) and ionization chambers (IBA CC13) were employed to measure PDD and crossline profile curves for all photon energies, including both FF and FFF beams.

The Blue phantom utilized in the measurements has dimensions of 48×48×48 cm^3. The ionization chambers used, specifically the CC13 model, has a volume of 0.13 cm^3, with the sensitive volume characterized by a inner diameter of 6.0 mm and a total active length of 5.8 mm.

Measurements were conducted at a source-to-surface distance (SSD) of 100 cm, employing square field sizes of 10×10 cm^2. The measurement grid utilized a step size of 0.1 cm, covering a depth range from 0 to 30 cm along the central axis for PDDs and along the axis perpendicular to the central axis of the radiation beam at a depth of 10 cm for profile measurements.

To facilitate data acquisition and control, the measurement system was connected to a computer and managed using the MyQAaccept software provided by the IBA company.

Simulation with Geant4/GATE

Flattened filter photon beams with energies of 6, 8, 10, and 15 MV, as well as unflattened beams with energies of 6 and 10 MV, were simulated to characterize percentage depth dose and off-axis distance profiles. The simulation conditions were configured to mirror those of the experimental measurements. The GATE platform version 9.1 was utilized for simulation, employing the Geant4 EM Standard Option 3 physical models to ensure precise dose calculation.

Phase Space files of the TrueBeam STx Linac photon beams provided by Varian were utilized to streamline the simulation process. These Phase Space data modeled the Linac head geometry upstream of the secondary collimators in a plane just above the secondary jaws. The downstream part of the Linac head was modeled based on drawings and specifications provided by Varian. The simulation of Linac head components and interaction of a photon in the water phantom on GATE are illustrated in Fig. 1.

A number of event of 2×10^9 was set in the GATE code. Photon and electron cut-off energies were adjusted to 0.05 MeV and 0.1 MeV, respectively, to optimize computing time during the simulation process. The size of the water tank phantom used in the simulation was 30×30×35 cm^3 (x × y × z), and a voxel size of 1×1×1 mm^3 was employed to calculate the PDDs on the central axis and the profiles.

The statistical uncertainty of Monte Carlo results was maintained at less than 1 %. Simulation results were extracted as image.img files, processed using ImageJ open-source software and presented in tabular form for analysis.

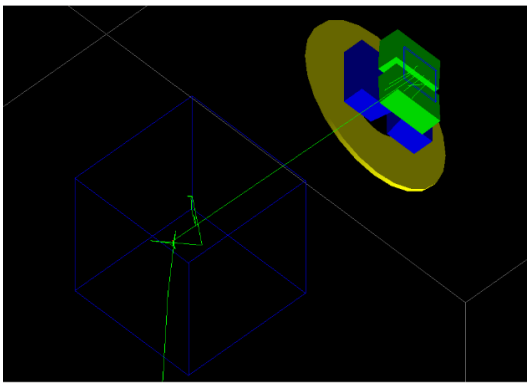

Fig. 1. Illustration of head Linac components and interaction of a photon in water phantom on GATE v9.1.

Gamma index method

The dose distribution of the PDD and beam profiles were simulated and compared to the experimental data using the Gamma Index method [11]. The Gamma Index method uses two separate criteria, the dose difference (DD) at a certain point and the distance-to-agreement (DTA) value, to determine the acceptability of the dose calculation, see Eq. (1).

$$\gamma = \sqrt{\frac{\Delta x^2}{DTA^2} + \frac{\Delta D^2}{DD^2}} \quad (1)$$

In this study, the Gamma Index method was applied with acceptance criteria of 1 %/1mm,2 %/2mm, and 3 %/3mm for the dose difference (DD) and the distance-to-agreement (DTA), respectively. These criteria were chosen to assess the agreement between simulated and experimental data. Additionally, the criteria proposed by the American Association of Physicists in Medicine (AAPM) of 2 %/2mm were also considered.

For each calculation point, Δx represents the distance between the reference point and the closest calculated point, while ΔD represents the dose difference between the simulated and measured doses at that point.

If the calculated Gamma Index (γ) is less than or equal to 1, the calculation point passes the test, indicating good agreement between simulated and measured data. Conversely, if γ is greater than 1, the calculation point fails the test, suggesting discrepancies between simulated and measured data.

Validation was conducted using a program written in Dev-C++ 5.11 code, which evaluated the percentage of points that passed the test, known as the gamma pass rate. This metric provides an overall assessment of the accuracy of the simulation results compared to experimental data.

Determine photon beam characteristics

Most of the dose characteristics of photon beams are determined on PDD and profile curves received from simulation results. For the unflattened beams, it is necessary to normalize the profile before calculating several beam characteristics, such as field size and penumbra. Different methods exist to normalize the FFF profile, such as using the inflection point [12] or shoulder point [13]. This work uses Pönisch's method to normalize the profiles, illustrated in Fig. 2.

In Fig. 2, the left ordinate axis depicts the dose of the flattened profile grey, and the right ordinate axis is the dose of the unflattened beam black. The inflection points of the unflattened profile D_u and the flattened profile D_f are used to renormalize the unflattened profile, see Eq. (2).

$$D_n = \frac{D_u}{D_f} \times D_{CAX} \quad (2)$$

where D_u is the dose at the inflection point of the penumbra region of the unflattened beam, D_f is the dose at the inflection point of the flattened profile, and D_{CAX} is the dose on the central axis of the flattened beam.

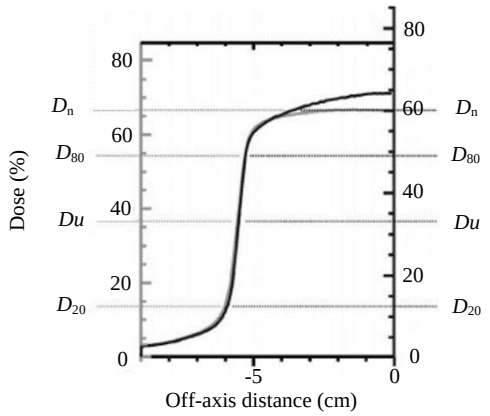

Fig. 2. Normalization of an unflattened profile of a photon beam.

Dose characteristics of photon beam are investigated:

The depth of maximum dose (d_{max}) along the central axis of a photon beam is a critical parameter in radiotherapy treatment planning, as it indicates the depth at which the highest dose is delivered within the patient's tissue. For Varian linac systems, the standard d_{max} values for various photon beams are as follows: 6 MV FF: 16 mm; 6 MV FFF: 14 mm; 8 MV FF: 19 mm; 10 MV FF: 26 mm; 10 MV FFF: 24 mm; 15 MV FF: 28 mm. These values represent the typical depths at which the maximum dose is reached along the central axis of the photon beam for each energy and filter configuration on the Varian linac system. They are derived from "golden beam data", which refers to benchmark data obtained through extensive calibration and validation processes to ensure accurate and reliable treatment delivery.

$TPR_{20/10}$: the tissue phantom ratio that represents beam quality. When one uses $TPR_{20/10}$ as a quality index (Qi), it is measured by the described $D_{20/10}$, the ratio of the dose at the isocenter in water at two different depths of 20 cm to a depth of 10 cm [14], see Eq. (3).

$$TPR_{20/10} = 1.2661 \times D_{20/10} - 0.0595 \quad (3)$$

Surface dose: the surface dose value of any field size is defined as the dose calculated at the surface of the medium divided by the dose at d_{max}. Following some research, the surface dose parameter is calculated at d = 0.5 mm [13,15], d = 1 mm [8], and d = 3 mm [16].

Dosimetric field size: For FF beam profiles, the field size is typically defined as the distance between points where the dose reaches 50 % of the maximum dose at a depth of 10 cm (d=10cm). This definition is commonly used for FF beams and provides a straightforward measure of the beam width.

However, when dealing with FFF beams, the profile must be normalized before calculating the field size. Due to the absence of a flattening filter, FFF profiles may exhibit irregularities that can affect the accuracy of field size determination if not normalized.

In the case of FFF beams, the dosimetric field size is defined as the distance between the right and left inflection points of the normalized profile. These inflection points represent the locations where the slope of the profile changes sign, indicating the transition from the central region to the penumbra region. By using the inflection points, the field size of FFF beams can be accurately determined, accounting for any irregularities in the profile shape.

This method ensures consistency in field size determination for both FF and FFF beams, allowing for reliable comparison and analysis of beam characteristics across different beam configurations [12].

Penumbra: In the context of a conventional flattened beam, the penumbra is commonly defined as the region between 20 % and 80 % of the central axis dose of the beam profile. This definition represents the transition region between the high-dose region (peak) and the low-dose region (fall-off) of the beam profile.

However, for unflattened beams, such as those generated in FFF mode, the profile must be normalized before determining the penumbra. The penumbra of an unflattened beam is defined as the distance between the positions of the 20 % and 80 % of the normalized dose (D_n) on the profile. This ensures that any irregularities in the profile shape are taken into account when measuring the penumbra width.

In this work, the final result for the penumbra width is obtained by selecting the maximum value of the left or right penumbra. This approach ensures that the widest part of the penumbra is considered, providing a comprehensive measure of the beam's spatial dose gradient.

Flatness: The flatness is used to evaluate the dose variation within the central beam region; it should be kept minimal. For the FF beam, flatness (F) is assessed by finding the maximum D_{max} and minimum D_{min} dose point values on the beam profile within 80 % of the beam width [17]. Beam flatness is defined as Eq. (4).

$$F = 100 \times \frac{D_{max} - D_{min}}{D_{max} + D_{min}} \quad (4)$$

where D_{max} is the maximum dose anywhere in the radiation field, D_{min} on 80 % of the beam profile [17].

For the FFF beams, the concept of flatness is different from that of FF beams, and the profile must be modified before calculating. Unflatness is the parameter relative to FFF beams corresponding to flatness for FF beams. The unflatness of the FFF beam can be defined as the ratio between the dose level at the beam central axis and the dose level on 80 % of the field region beam [13], see Eq. (5).

$$\text{Unflatness} = D_{CAX}/D_{off-axis} \quad (5)$$

where D_{CAX} is the dose at the central axis, the $D_{off-axis}$ is the dose at the 80 % field size.

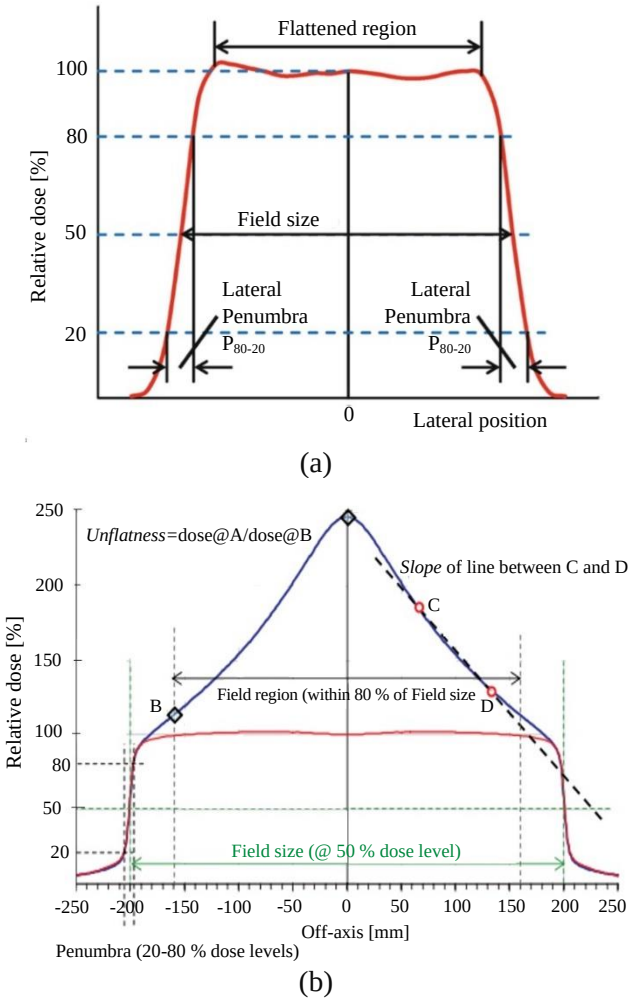

Fig. 3. Illustration of FF, FFF beam profile and parameters. (a) The FF beam profile and parameters: field size, penumbra, flattened region [18]. (b) Description of some of the FFF beam parameters: field region, field size, penumbra, unflatness (Point A: central axis; point B: off-axis at 80 % of the field size) [13].

Symmetry: Symmetry (S) determines the degree of equality level between the left and right sides of a profile; it can be defined as usual for standard FF beam, with the only difference that the evaluation area should be within the field region for FFF beams instead of the flattened region commonly used in FF beams [19,20], see Eq. (6).

$$S = \left(\left|\frac{Point\ L}{Point\ R}\right|, \left|\frac{Point\ R}{Point\ L}\right|\right) \quad (6)$$

where Point L and Point R are points on the left and right side of the profile equidistant from the central axis within the flattened region defined as 80 % of the field width [20]. The FF, FFF photon beam profiles and parameters are illustrated in Fig. 3.

RESULTS AND DISCUSSION

Validation of PDD and profile

Theoretically, in the FFF beam mode without a flattened filter, the PDD is expected to exhibit shallower depth compared to an FF beam. This is primarily due to the softer energy spectra of photons in the FFF beam, which results in reduced attenuation as the beam penetrates into the tissue. Additionally, the beam profile of an FFF beam typically displays a bell-shaped distribution, reflecting the characteristics of the beam energy spectrum [21].

Experimental measurements and simulations have consistently shown results that support this theoretical expectation. Validation of PDD and beam profile data involves comparing simulated results with experimental measurements. This comparison is typically performed using the Gamma Index method, which evaluates the agreement between simulated and measured data based on predefined criteria for DD and DTA.

Table 1. Comparison of GATE and measurement on PDD and profile of FF, FFF photon beams using Gamma Index method.

Beam		Gamma pass rate (%)		
		1mm/1 %	2mm/2 %	3mm/3 %
PDD	6 X	95	98	100
	6 FFF	94	97	100
	10 X	94	97	100
	10 FFF	96	99	100
	8 X	95	98	100
	15 X	94	97	99
Profile	6 X	93	95	99
	6 FFF	92	95	98
	10 X	95	98	100
	10 FFF	95	98	100
	8 X	94	97	100
	15 X	90	94	97

(where X stand for MV FF, FFF stand for MV FFF)

The validation results, expressed as the Gamma pass rate, provide insights into the accuracy of the simulation model in replicating experimental measurements. Table 1 lists the Gamma pass rates

obtained using criteria of 1mm/1 %, 2mm/2 %, and 3mm/3 % for DD and DTA, respectively. These values indicate the percentage of points in the PDD and profile curves that passed the Gamma Index test, demonstrating acceptable agreement between simulated and experimental data within the specified tolerances Table 1.

Figures (4,5) illustrate the result of PDDs and the profile photon beams on the Truebeam STx linac simulated on the GATE platform and measured experimentally, including 4 FF beams (6, 8, 10, 15 MV), 02 FFF beams (6, 10 MV).

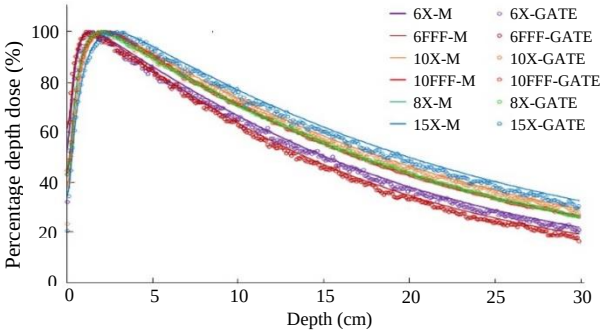

Fig. 4. Comparison of the PDD of FF, FFF photon beams between GATE and measurement for 10 × 10 cm^2 field size.

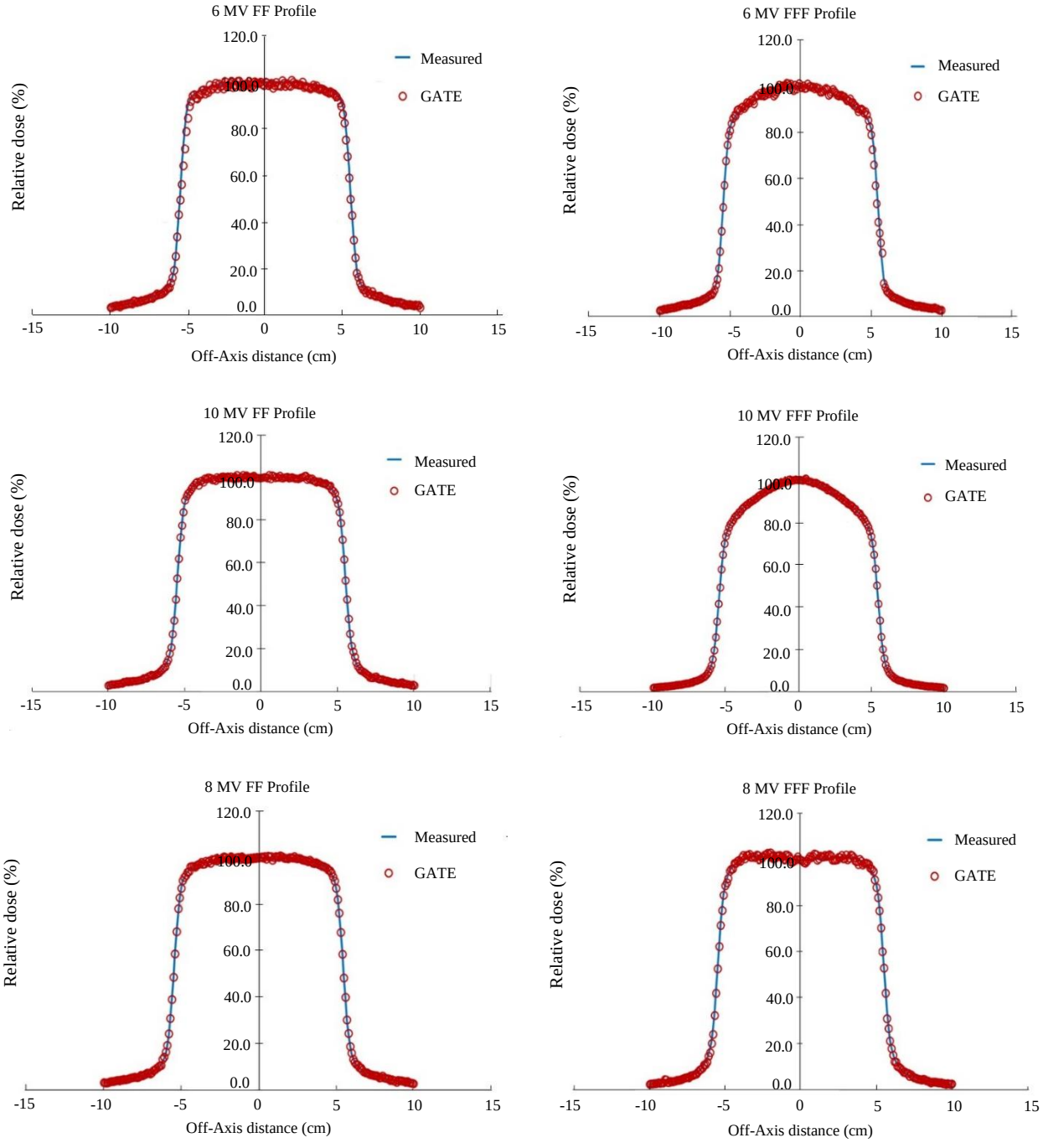

Fig. 5. Comparison of cross-profile of FF, FFF photon beams between GATE and measurement, field size 10 × 10 cm^2 at 10 cm depth.

The comparison between GATE Monte Carlo simulation results and experimental measurements using the Gamma Index method demonstrates good agreement. For PDD curves, the gamma pass rates were nearly 100 % for the 3 %/3mm criterion, with the exception of the 15 MV FF beam, which achieved a 99 % pass rate. When using the 2 %/2mm criterion, the gamma pass rates were over 95 % for all beams. However, for the 1 %/1mm criterion, the gamma pass rates were mostly less than 95 % but still exceeded 90 %.

Similarly, for profile curves, the gamma pass rates were lower compared to PDD curves across all criteria, particularly for the 15 MV profile. Despite this, more than 90 % of the points for all simulations passed the 1 %/1mm gamma criterion. Notably, with the criteria proposed by the AAPM of 2 %/2mm, the validation results were in agreement.

These results indicate that the GATE Monte Carlo simulation accurately reproduces the experimental measurements for both PDD and profile curves, with minor discrepancies observed primarily at stricter gamma criteria. Overall, the validation results provide confidence in the accuracy and reliability of the simulation model for assessing photon beam characteristics on the TrueBeam STx linac.

Investigate the photon beam characteristics

Dosimetric characteristics of photon beams are studied beyond the PDD (d_{max}, $TPR_{20/10}$, surface dose) and profile curve (field size, penumbra, flatness, and symmetry).

The maximum dose depth (d_{max}) is primarily influenced by the energy of the photon beam. Typically, d_{max} values for individual linacs fall within a general range corresponding to their nominal energy values. However, differences in d_{max} can also be observed between linac generations from different manufacturers, such as Varian and Elekta.

For the Varian TrueBeam series, typical dmax values are as follows: 6 MV FF: 16 mm; 6 MV FFF: 14 mm; 8 MV FF: 19 mm; 10 MV FF: 26 mm; 10 MV FFF: 24 mm; 15 MV FF: 28 mm. These values are derived from "golden beam data" and are indicative of the expected d_{max} values for each energy level. The acceptable tolerance for d_{max} is typically set at 2 mm.

In this study, the calculated d_{max} values were generally smaller than the experimental measurements, with differences mainly ranging from 1 mm to 2 mm. The largest discrepancy was observed for the 15 MV FF beam, with a clearance of 2 mm. Despite these differences, the calculated values remained within an acceptable tolerance range.

Alternatively, beam quality in radiotherapy can be evaluated using the Tissue Phantom Ratio (TPR) value, specifically $TPR_{20/10}$. Higher energy beams typically exhibit better $TPR_{20/10}$ values, and FFF beams usually have smaller $TPR_{20/10}$ values compared to FF beams of the same energy level.

Table 2 presents the agreement between simulation and measurement for $TPR_{20/10}$ values, with percentage differences consistently smaller than 3 %. This indicates good agreement between simulated and measured values, further supporting the accuracy of the simulation model in characterizing beam quality.

Surface dose, defined as the percentage of the dose relative to the dose at d_{max}, is a critical parameter in radiotherapy treatment planning. It represents the dose received by the surface of the irradiated target and is influenced by various factors, including scattered photons from collimators and filters, backscattered photons from the phantom, and high-energy electrons produced by photon interactions [17].

In general, surface dose tends to be much lower than the maximum dose at d_{max}. However, it increases with decreasing beam energy, and for a given energy level, the surface dose is typically higher for FFF beams compared to FF beams.

Table 2. Comparison of the beam qualities (d_{max}, $TPR_{20/10}$) of the FF, FFF photon beams between GATE and measurement.

Beam	d_{max} (mm)			$TPR_{20/10}$		
	Measured	GATE	Diff	Measured	GATE	Diff (%)
6 X	15	14	-1	0.6670	0.6669	-0.0114
6 FFF	14	13	-1	0.6324	0.6165	-2.5764
10 X	24	23	-1	0.7398	0.7507	1.4528
10 FFF	23	23	0	0.7080	0.7064	-0.2316
8 X	19	20	1	0.7116	0.7273	2.1557
15 X	27	25	-2	0.7653	0.7467	-2.4929

Maximum dose depth, d_{max} [cm]
Quality index (Qi), $TPR_{20/10}$

Table 3. Comparison of the surface dose of the FF, FFF photon beams between GATE and measurement at different depths.

Beam	Surface dose								
	0.5 mm			1 mm			3 mm		
	Measured	GATE	% Diff	Measured	GATE	% Diff	Measured	GATE	% Diff
6 X	56.35	51.79	-8.09	59.10	56.60	-4.23	75.70	72.79	-3.84
6 FFF	63.21	58.47	-7.50	65.21	63.81	-2.15	79.40	82.19	3.51
10 X	39.75	36.81	-7.40	41.90	40.60	-3.10	57.48	59.63	3.74
10 FFF	46.91	46.73	-0.38	48.92	48.80	-0.25	64.08	64.06	-0.02
8 X	45.25	45.45	0.44	47.20	47.79	1.25	62.56	64.24	2.68
15 X	36.13	33.37	-7.64	37.87	36.08	-4.73	52.50	53.73	2.34

The results presented in Table 3 demonstrate that the surface dose at depths of 0.5 mm and 1 mm for FFF beams is significantly higher than that for FF beams at the same energy level. The largest difference between simulation and measurement results is observed at 0.5 mm depth for the 6 MV FF beam, with the remaining differences generally below 8.1 %.

It is important to note that the significant discrepancy observed, particularly at 0.5 mm depth, may be attributed to the method of experimental measurement. Although cylindrical ionization chambers are commonly employed for PDD curve measurements, it is recommended to use parallel-plate ionization chambers for surface dose measurements to enhance accuracy. Despite these guidelines, our study utilized cylindrical ionization chambers for measuring surface dose.

Overall, these results underscore the importance of accurate surface dose measurements and highlight the potential impact of measurement techniques on the reliability of experimental data in radiotherapy dosimetry.

In accordance with standard photon beam specifications, various dosimetric parameters such as field size, penumbra, flatness, and symmetry are typically measured in a water phantom at a depth of d = 10 cm, with a Source-to-Surface Distance (SSD) of 100 cm and a field size of 20 × 20 cm^2. However, for the sake of convenience and comparison, this study opts for a standard field size of 10 × 10 cm^2 for both experimental measurements and simulations.

Using a standardized field size facilitates direct comparison between measured and simulated data, ensuring consistency in the evaluation of dosimetric parameters across different studies and treatment facilities. Additionally, a field size of 10 × 10 cm^2 is commonly used in clinical practice and provides a representative sample of beam characteristics for various treatment scenarios.

By employing the same field size for both measurements and simulations, any observed differences in dosimetric parameters can be attributed more confidently to variations in beam properties rather than differences in measurement conditions. This approach enhances the reliability and validity of the comparative analysis, enabling a more accurate assessment of the performance of the simulation model in replicating experimental data.

Table 4 presents the dosimetric field size results obtained from cross-profile measurements. For FFF beams, these results are recorded on the profile after normalization. It is evident that the field size of the FFF beam is not substantially smaller than that of the FF field in the simulation.

The comparison between simulation and experimental measurement results reveals that there is no significant difference in the field size. The discrepancy observed is less than or equal to 0.2 cm, which corresponds to approximately 2 % of the 10 × 10 cm^2 field size.

This close agreement between simulation and measurement indicates that the simulation model accurately replicates the field size characteristics of the photon beams. The small error observed further reinforces the reliability of the simulation data and demonstrates the effectiveness of the simulation approach in assessing dosimetric parameters.

Table 5 compares the penumbra values calculated using GATE simulation with experimental measurements. In this study, the penumbra width is calculated at a depth of 10 cm and for a field size of 10 × 10 cm^2, with the maximum value obtained from either the left or right penumbra.

Table 4. Comparison of the dosimetric field size of the FF, FFF photon beams between GATE and measurement.

Beam	Field size (cm)		
	Measured	GATE	Diff
6 X	11.0	11.0	0.0
6 FFF	10.9	10.7	-0.2
10 X	11.0	11.0	0.0
10 FFF	10.8	10.7	-0.1
8 X	11.0	10.9	-0.1
15 X	11.0	11.0	0.0

Table 5. Comparison of the penumbra of the FF, FFF photon beams between GATE and measurement.

Beam	Penumbra (mm)		
	Measured	GATE	Diff
6 X	9.0	9.0	0.0
6 FFF	9.0	10.0	1.0
10 X	10.0	10.5	0.5
10 FFF	11.5	13.0	1.5
8 X	7.0	8.0	1.0
15 X	8.0	8.0	0.0

For FFF beams, the average penumbra is reported to be slightly smaller than that of FF beams, but the difference is typically less than 1 mm [12].

The results indicate that the 10 MV FFF photon beam recorded the most significant penumbra widths of 11.5 mm and 13.0 mm for measurement and simulation, respectively. The penumbra value for the 10 MV FFF photon beam is also similar to the findings of a previous study by Muralidhar et al. [22].

It is noteworthy that most of the simulation results exhibit wider penumbra widths compared to the measurements, with the most significant difference being approximately 1.5 mm. This discrepancy suggests a slight overestimation of penumbra width in the simulation compared to the actual measurements. Further investigation may be warranted to identify potential sources of this discrepancy and refine the simulation model for improved accuracy in predicting penumbra characteristics.

Table 6 presents the flatness results for FF photon beams and the degree of unflatness for FFF beams. It is expected that the flatness of FF photon beams and the degree of unflatness for FFF beams should be less than 3 % [13,17].

The results demonstrate that all flatness values fall within the specified tolerance range. Both the simulated and experimental measurements show good agreement, with the maximum flatness error observed at 2.971 % for the 6 MV FF beam simulation.

This consistency between simulation and measurement highlights the accuracy of the simulation model in replicating measurement of the flatness characteristics of the photon beams. The small discrepancies observed underscore the importance of precise calibration and validation processes to ensure reliable dosimetric data for radiotherapy treatment planning. Overall, the agreement between simulation and measurement results provides confidence in the reliability of the simulation approach for assessing flatness in photon beams.

Table 7 compares the symmetry values between measurements and simulations, with the expectation that the symmetry of the photon beam should be less than 106 % [19,20]. The results indicate good agreement between the simulation and experimental measurements, with slight differences ranging from 0.7 % to 2.9 %. The most significant deviation is observed for the 6 MV FFF photon beam, with a difference of 2.9 %.

Despite these small discrepancies, the overall agreement between simulation and measurement results suggests that the simulation model effectively replicates the symmetry characteristics of the photon beams. It is common for slight variations to occur between simulated and measured values due to factors such as experimental conditions, uncertainties in measurement devices, and modeling assumptions in the simulation.

Nevertheless, the consistency observed between simulation and measurement results reaffirms the reliability of the simulation approach for assessing beam symmetry in photon beams. These findings contribute to the validation of the simulation model and provide confidence in its accuracy for dosimetric evaluations in radiotherapy treatment planning.

Table 6. Comparison of the flatness of the FF, FFF photon beams between GATE and measurement.

Beam	Flatness (%)		
	Measured	GATE	Diff
6 X	1.637	2.971	1.334
10 X	1.323	1.908	0.585
8 X	1.712	2.066	0.354
15 X	0.960	2.550	1.590
	Unflatness		
6 FFF	1.129	1.107	-0.022
10 FFF	1.213	1.215	0.002

Table 7. Comparison of the symmetry of the FF, FFF photon beams between GATE and measurement.

Beam	Symmetry (%)		
	Measured	GATE	Diff
6 X	100.2	102.4	2.2
6 FFF	100.2	103.1	2.9
10 X	100.5	101.2	0.7
10 FFF	100.1	101.1	1.0
8 X	100.4	101.4	1.0
15 X	100.3	104.0	3.7

CONCLUSION

The results obtained from using the Geant4/GATE simulation toolkit to model and investigate the characteristics of the photon beam on the TrueBeam STx linac demonstrate several key findings:

Agreement with Experimental Measurements: The simulation results exhibit good agreement with experimental measurements for both PDD and off-axis distance profile. While the Gamma Index shows slightly lower agreement with stricter criteria, the gamma pass rate remains consistently above 90 % for all beams, indicating acceptable agreement between simulation and measurement.

Dosimetric Characteristics: The dosimetric characteristics of the photon beam obtained from simulation closely match the measured values.

Parameters such as d_{max}, $TPR_{20/10}$, dosimetric field size, penumbra, flatness, and symmetry show no significant differences between simulation and measurement. However, there is a notable difference in the surface dose parameter for the 6 MV FF beam at a depth of 0.5 mm, with a discrepancy of 3.83 %. Despite this, all other parameters exhibit differences of less than 3 %, indicating good agreement overall.

Suitability of Geant4/GATE Simulation Toolkit: The results suggest that the Geant4/GATE simulation toolkit is suitable for accurately modeling and investigating the photon beam characteristics of the TrueBeam STx accelerator. The toolkit provides reliable results that closely align with experimental measurements, indicating its efficacy for dosimetric evaluations in radiotherapy treatment planning.

Overall, these findings affirm the utility and effectiveness of using simulation tools such as Geant4/GATE for studying and optimizing the performance of radiation therapy equipment, contributing to enhanced treatment planning and delivery processes.

ACKNOWLEDGMENT

We would like to thank the Department of Radiation Oncology and Radiosurgery, 108 Military Central Hospital, for supporting this work.

AUTHOR CONTRIBUTION

Pham Hong Lam and Pham Quang Trung wrote the manuscript and performed simulations on GATE and experimental measurements on the Linac. Phan Tien Dung and Pham Quang Trung came up with ideas and directions for conducting the research.

REFERENCES

1. J. Gao and X. Liu, Int. J. Med. Phys. Clin. Eng. Radiat. Oncol. **8** (2019) 20.
2. K. R. Mani, M. A. Bhuiyan, M. S. Rahman *et al.*, Pol. J. Med. Phys. Eng. **24** (2018) 79.
3. J. Seco and F. Verhaegen, Monte Carlo Techniques in Radiation Therapy, 2nd ed., CRC Press, Boca Raton (2022) 1.
4. R. Sapundani, R. Ekawati and K. M. Wibowo, Atom Indones. **47 (**2021) 199.
5. B. T. Hung, T. T. Duong and B. N. Ha, Atom Indones. **49** (2023) 13.
6. D. Sarrut, M. Bardies, N. Boussion *et al*., Med. Phys. **41** (2014) 064301-1.
7. A. Mesbahi, P. Mehnati and A. Keshtkar, Iran. J. Radiat. Res. **5** (2007) 23.
8. M. Mohammed, E. Chakir, H. Boukhal *et al*., J. King Saud Univ. Sci. **29** (2017) 371.
9. E. Gündem and B. Dirican, Radiat. Phys. Chem. **184** (2021) 109491.
10. A. Sara, M. E. A. Krabch and M. Trihi, Oncol. Radiother. **16** (2022) 22.
11. D. A. Low, W. B. Harms, S. Mutic *et al*., Med. Phys. **25** (1998) 656.
12. F. Pönisch, U. Titt, O. N. Vassiliev *et al*., Med. Phys. **33** (2006) 1738.
13. A. Fogliata, R. Garcia, T. Knöös *et al*., Med. Phys. **39** (2012) 6455.
14. D. S. Followill, R. C. Tailor, V. M. Tello *et al*., Med. Phys. **25** (1998) 1202.
15. S. F. Kry, S. A. Smith, R. Weathers *et al.*, J. Appl. Clin. Med. Phys. **13** (2012) 20.
16. O. N. Vassiliev, U. Titt, F. Pönisch *et al.*, Phys. Med. Biol. **51** (2006) 1907.
17. E. B. Podgorsak, Radiation Oncology Physics: A Handbook for Teachers and Students, International Atomic Energy Agency, Vienna (2005) 1.
18. S. Kamizawa, *Quality Assurance for Proton Beam Radiotherapy*, in: Proton Beam Radiotherapy, Springer, Singapore (2020) 139.
19. IEC, Medical Electrical Equipment - Medical Electron Accelerators - Functional Performance Characteristics, 2nd ed., International Electro-technical Commission (IEC 60976), Geneva (2007) 1.
20. M. Joan, S. Saminathan, R. Manickam *et al*., J. Phys. Conf. Ser. **1248** (2019) 012037.
21. Y. Xiao, S. F. Kry, R. Popple *et al.*, J. Appl. Clin. Med. Phys. **16** (2015) 12.
22. K. Muralidhar, B. K. Rout, K. Ramesh *et al.*, J. Cancer Res. Ther. **11** (2015) 136.